

Discretisation Details for a Pressure-Based Co-located Finite Volume Solution Method with Temperature–Velocity Coupling

S. Vakilipour

S.J. Ormiston

University of Manitoba

Department of Mechanical Engineering

75A Chancellors Circle, Winnipeg, Manitoba

Canada, R3T 5V6

Technical Report CTFSRG-TR-01-2011

July 2011 (Rev. A: 2012-09-02)

1 Governing Equations

The governing equations are written for conservation of mass, momentum, and energy of two-dimensional Newtonian fluid flow. It has been assumed that the flow is steady, laminar, and incompressible with negligible viscous dissipation and pressure work source terms in the energy equation. Radiation heat transfer is also neglected. The Boussinesq approximation has been applied to model the buoyancy force terms in the momentum equations. The equations for conservation of mass, momentum, and energy are written as:

$$\frac{\partial}{\partial x}(\rho U) + \frac{\partial}{\partial y}(\rho V) = 0 \quad (1)$$

$$\frac{\partial}{\partial t}(\rho U) + \frac{\partial}{\partial x}(\rho UU) + \frac{\partial}{\partial y}(\rho VU) = -\frac{\partial P}{\partial x} + \frac{\partial}{\partial x}\left(\mu \frac{\partial U}{\partial x}\right) + \frac{\partial}{\partial y}\left(\mu \frac{\partial U}{\partial y}\right) + \rho g_x \beta (T - T_{\text{ref}}) \quad (2)$$

$$\frac{\partial}{\partial t}(\rho V) + \frac{\partial}{\partial x}(\rho UV) + \frac{\partial}{\partial y}(\rho VV) = -\frac{\partial P}{\partial y} + \frac{\partial}{\partial x}\left(\mu \frac{\partial V}{\partial x}\right) + \frac{\partial}{\partial y}\left(\mu \frac{\partial V}{\partial y}\right) + \rho g_y \beta (T - T_{\text{ref}}) \quad (3)$$

$$\frac{\partial}{\partial t}(\rho T) + \frac{\partial}{\partial x}(\rho UT) + \frac{\partial}{\partial y}(\rho VT) = \frac{\partial}{\partial x}\left(\frac{k}{C_p} \frac{\partial T}{\partial x}\right) + \frac{\partial}{\partial y}\left(\frac{k}{C_p} \frac{\partial T}{\partial y}\right) \quad (4)$$

The transient terms have been retained in Eqs. (2) to (4) to allow relaxation in the iteration toward the steady-state solution.

2 Discretisation of the Governing Equations

A finite volume method [1] is used to discretise the governing differential equations. Equations (1) to (4) are integrated over a typical control volume centred at P as shown in Figure 1. For each face of the typical control volume, the mass flow rate is determined using the face velocities, which are determined at the integration point (ip) at the centre of the face (denoted by e , w , n , and s in Figure 1). Other fluxes are determined using the face value and gradient of the dependent variables evaluated at the integration points. All fluxes computed at an ip are assumed constant along the face. All unknowns are located at cell centres and the values at ne , nw , se , and sw corners in Figure 1 are estimated by linear interpolation.

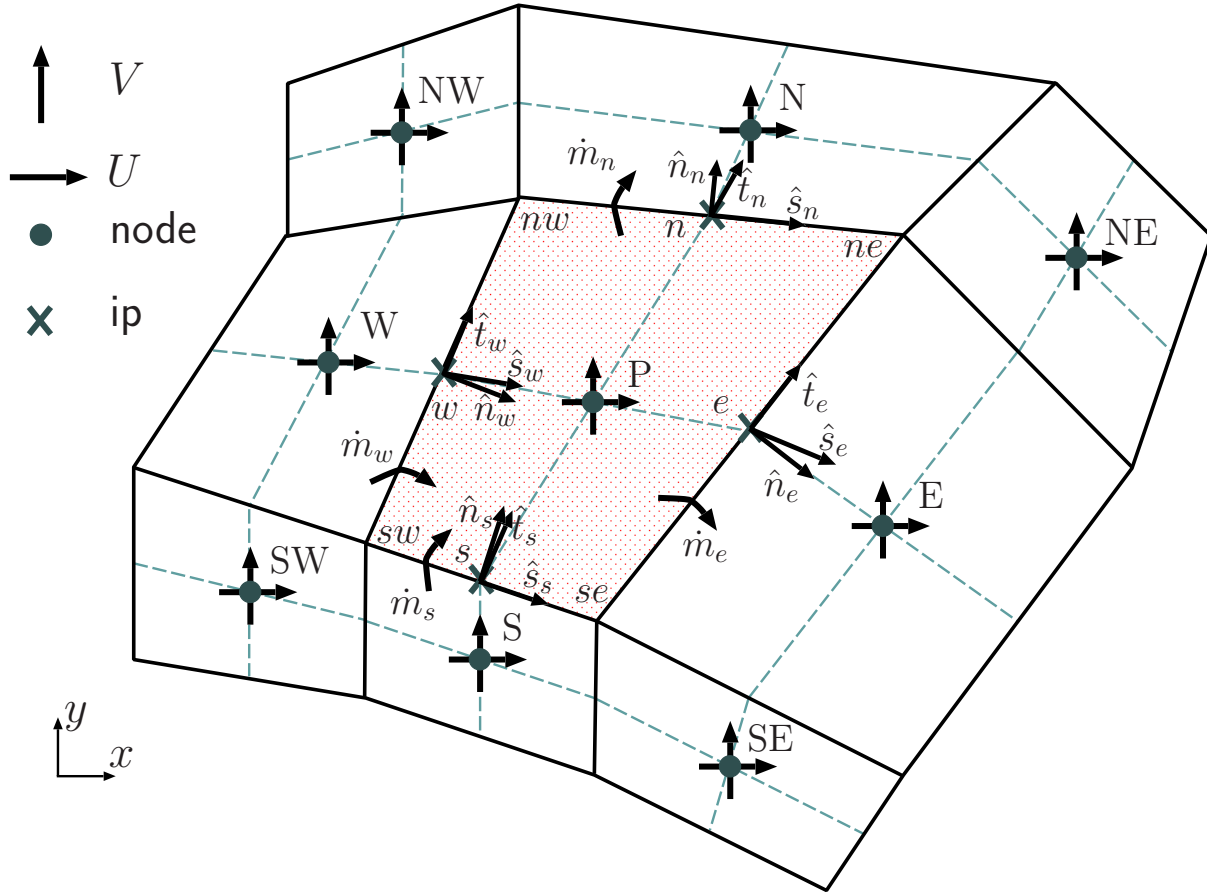


Figure 1: Control volume nomenclature

The level 1 discretisation of Equations (1) to (4) yields the following algebraic equations for conservation of mass, momentum, and energy, respectively.

$$\dot{m}_e - \dot{m}_w + \dot{m}_n - \dot{m}_s = 0 \quad (5)$$

$$\begin{aligned} & \frac{(\rho \mathcal{V}_P)}{\Delta t} (U_P - U_P^o) + \dot{m}_e U_e - \dot{m}_w U_w + \dot{m}_n U_n - \dot{m}_s U_s = \\ & - \frac{\partial P}{\partial x} \Big|_P \mathcal{V}_P + D_e^u \frac{\partial U}{\partial n} \Big|_e - D_w^u \frac{\partial U}{\partial n} \Big|_w + D_n^u \frac{\partial U}{\partial n} \Big|_n - D_s^u \frac{\partial U}{\partial n} \Big|_s + \rho g_x \beta (T_P - T_{\text{ref}}) \mathcal{V}_P \end{aligned} \quad (6)$$

$$\begin{aligned} & \frac{(\rho \mathcal{V}_P)}{\Delta t} (V_P - V_P^o) + \dot{m}_e V_e - \dot{m}_w V_w + \dot{m}_n V_n - \dot{m}_s V_s = \\ & - \frac{\partial P}{\partial x} \Big|_P \mathcal{V}_P + D_e^v \frac{\partial V}{\partial n} \Big|_e - D_w^v \frac{\partial V}{\partial n} \Big|_w + D_n^v \frac{\partial V}{\partial n} \Big|_n - D_s^v \frac{\partial V}{\partial n} \Big|_s + \rho g_y \beta (T_P - T_{\text{ref}}) \mathcal{V}_P \end{aligned} \quad (7)$$

$$\begin{aligned} & \frac{(\rho \mathcal{V}_P)}{\Delta t} (T_P - T_P^o) + \dot{m}_e T_e - \dot{m}_w T_w + \dot{m}_n T_n - \dot{m}_s T_s = \\ & D_e^t \frac{\partial T}{\partial n} \Big|_e - D_w^t \frac{\partial T}{\partial n} \Big|_w + D_n^t \frac{\partial T}{\partial n} \Big|_n - D_s^t \frac{\partial T}{\partial n} \Big|_s \end{aligned} \quad (8)$$

In the development of the coupled algebraic equations, unsuperscripted dependent variables indicate values at the new time step level. Note that velocity-to-temperature coupling is introduced by the use of T_P in Eqs. (6) and (7).

In level 2 of the discretisation, the mass flow rates, the face values in the advection terms, and the derivatives must be approximated appropriately. The mass flow rate at a face is calculated as:

$$\dot{m}_f = \rho A_f \left(\vec{\mathbf{V}}_f \cdot \hat{\mathbf{n}}_f \right) = \rho A_f \left(\hat{U}_f n_{f,x} + \hat{V}_f n_{f,y} \right) \quad (9)$$

where the face velocity components are \hat{U} and \hat{V} and $n_{f,x}$ $n_{f,y}$ are the components of the normal unit vector on the face. The normal unit vectors at faces are shown in Figure 1.

A momentum interpolation scheme referred to here as the Pressure-Weighted Interpolation Method (PWIM) is used to estimate the face velocities in Eq. (9). The PWIM used in this work is based on the work of Rhie and Chow [2] and is similar to the approach described by Yu *et al.* [3]. It is formulated so that the converged solution is independent of the time step size. The PWIM estimations of the face velocity components are:

$$\hat{U}_f = \mathcal{W}_f U_P + (1 - \mathcal{W}_f) U_F - \hat{d}_f^u \frac{\partial P}{\partial x} \Big|_f + \tilde{b}_f^u \quad (10)$$

$$\hat{V}_f = \mathcal{W}_f V_P + (1 - \mathcal{W}_f) V_F - \hat{d}_f^v \frac{\partial P}{\partial y} \Big|_f + \tilde{b}_f^v \quad (11)$$

where

$$\tilde{b}_f^u = \hat{d}_f^u \left\{ \mathcal{W}_f \frac{\partial P}{\partial x} \Big|_P + (1 - \mathcal{W}_f) \frac{\partial P}{\partial x} \Big|_F \right\} + \frac{\rho}{\Delta t} \hat{d}_f^u \left\{ \hat{U}_f^o - \left[\mathcal{W}_f U_P^o + (1 - \mathcal{W}_f) U_F^o \right] \right\} \quad (12)$$

$$\tilde{b}_f^v = \hat{d}_f^v \left\{ \mathcal{W}_f \frac{\partial P}{\partial y} \Big|_P^o + (1 - \mathcal{W}_f) \frac{\partial P}{\partial y} \Big|_F^o \right\} + \frac{\rho}{\Delta t} \hat{d}_f^v \left\{ \hat{V}_f^o - \left[\mathcal{W}_f V_P^o + (1 - \mathcal{W}_f) V_F^o \right] \right\} \quad (13)$$

$$\hat{d}_f^\phi = \mathcal{V}_f \left\{ \frac{\mathcal{W}_f}{\left(a_P^{\phi, \phi} \right)_P} + \frac{(1 - \mathcal{W}_f)}{\left(a_P^{\phi, \phi} \right)_F} \right\} \quad (14)$$

In Eqs. (10) to (14), $F = \{E, W, N, S\}$ corresponding to $f = \{e, w, n, s\}$, and \mathcal{W}_f is a geometric linear interpolation factor at the face separating two adjacent nodes at P and F. The factor \mathcal{W}_f is computed using the distances from the integration point to the centres of the two adjacent nodal points; it is equal to 0.5 for a uniformly spaced mesh. The grid weights are given in Section 4.

In order to compute \mathcal{V}_f in Eq. (14), each control volume is divided into quadrants by lines connecting the integration points e to w and n to s as shown in Figure 1. The volume at an integration point, \mathcal{V}_f , is the summation of the volumes of the quadrants in control volumes for nodes P and F which are adjacent to the face f .

Eqs. (10) and (11) have been written to contrast the active nodal velocity and face pressure gradient terms that lead to the coupled algebraic equations versus the lagged terms which are given in Eqs. (12) and (13). The pressure gradients at faces in Eqs. (10) and (11) are evaluated using the appropriate combination of co-ordinate derivatives $(\frac{\partial x}{\partial s}, \frac{\partial x}{\partial t}, \frac{\partial y}{\partial s}, \frac{\partial y}{\partial t})$ and derivatives of pressure in the \hat{s} and \hat{t} directions (shown in Figure 1). The derivatives in the \hat{s} and \hat{t} directions create connections to the six nodal pressures surrounding each face f . Therefore, the discretisation of Eq. (5) produces implicit connections to five U nodes, five V nodes, and nine P nodes. The pressure gradients at control volume centres in Eqs. (6), (7), (12), and (13), on the other hand, are determined from face pressures which are computed by geometric interpolation using surrounding nodal values.

The advection terms in Eqs. (6) and (7) are made linear using mass flow rates from the previous time step:

$$\dot{m}_f U_f = \dot{m}_f^o U_f \quad (15)$$

$$\dot{m}_f V_f = \dot{m}_f^o V_f \quad (16)$$

The advection terms in Eq. (8), however, are approximated by a Newton-Raphson linearisation as in [4]:

$$\dot{m}_f T_f = \dot{m}_f^o T_f + \dot{m}_f T_f^o - \dot{m}_f^o T_f^o \quad (17)$$

The new iteration level mass flow rates in the second term on the right hand side of Eq. (17) are treated in the same way as the mass flow rates in continuity: they are evaluated using Eqs. (9) to (14). This linearisation and the use of the PWIM-based mass flow rates introduces implicit connections to nodal velocities and pressures into the algebraic equation for the temperature. This procedure produces implicit temperature-to-velocity coupling.

Finally, the face values of the dependent variable (ϕ_f) and its derivative in the diffusion terms $(\frac{\partial \phi}{\partial n} \Big|_f)$ are approximated in terms of nodal values. The advected scalars at the faces are estimated using an approximation to the exponential differencing scheme as proposed by

Raithby [5]. Gradients at faces are calculated by linear interpolation and have a diffusion weighting coefficient applied to them as in [5]. The details are given below.

$$\phi_e = (0.5 + \alpha_e) \phi_P + (0.5 - \alpha_e) \phi_E \quad (18)$$

$$\phi_w = (0.5 + \alpha_w) \phi_W + (0.5 - \alpha_w) \phi_P \quad (19)$$

$$\phi_n = (0.5 + \alpha_n) \phi_P + (0.5 - \alpha_n) \phi_N \quad (20)$$

$$\phi_s = (0.5 + \alpha_s) \phi_S + (0.5 - \alpha_s) \phi_P \quad (21)$$

The convective weight coefficients at each face, α_f , are computed as a function of the local Peclet number using the approximation to the exponential differencing scheme proposed by Raithby [5].

$$\alpha = \frac{1}{2} \left(\frac{\text{Pe}^2}{(5 + \text{Pe}^2)} \right) \quad (22)$$

To get the correct sign on α (it should carry the sign of the mass flow), use:

$$\alpha = \alpha \frac{|\dot{m}|}{\dot{m}} \quad (23)$$

Gradients at faces are calculated by linear interpolation. For example, at the east face:

$$\left. \frac{\partial \phi}{\partial s} \right|_e = \beta_e \frac{(\phi_E - \phi_P)}{(\delta s)_e} \quad (24)$$

More details of gradient calculations are given in Section 6.

The diffusion weighting factor, β_f , applied as in [5]:

$$\beta = \frac{(1 + 0.005 \text{Pe}^2)}{(1 + 0.05 \text{Pe}^2)} \quad (25)$$

Following the discretisation procedure described above, the final form of the linearised set of coupled algebraic equations for conservation of momentum, mass, and energy can be written as:

$$a_P^{u,u} U_P + \sum a_{\text{NB8}}^{u,u} U_{\text{NB8}} + a_P^{u,p} P_P + \sum a_{\text{NB4}}^{u,p} P_{\text{NB4}} + a_P^{u,t} T_P = b_P^u \quad (26)$$

$$a_P^{v,v} V_P + \sum a_{\text{NB8}}^{v,v} V_{\text{NB8}} + a_P^{v,p} P_P + \sum a_{\text{NB4}}^{v,p} P_{\text{NB4}} + a_P^{v,t} T_P = b_P^v \quad (27)$$

$$a_P^{p,p} P_P + \sum a_{\text{NB8}}^{p,p} P_{\text{NB8}} + a_P^{p,u} U_P + \sum a_{\text{NB4}}^{p,u} U_{\text{NB4}} + a_P^{p,v} V_P + \sum a_{\text{NB4}}^{p,v} V_{\text{NB4}} = b_P^p \quad (28)$$

$$a_P^{t,t} T_P + \sum a_{\text{NB8}}^{t,t} T_{\text{NB8}} + a_P^{t,u} U_P + \sum a_{\text{NB4}}^{t,u} U_{\text{NB4}} + a_P^{t,v} V_P + \sum a_{\text{NB4}}^{t,v} V_{\text{NB4}} + a_P^{t,p} P_P + \sum a_{\text{NB8}}^{t,p} P_{\text{NB8}} = b_P^t \quad (29)$$

The first and second superscripts of the a coefficients refer to the equation label and the multiplied variable, respectively. In summations, NB4={E,W,N,S} and NB8={NB4,NE, NW, SE,SW}. The details of the summations are:

$$\sum a_{\text{NB4}}^{e,\phi} \Phi_{\text{NB4}} = a_E^{e,\phi} \Phi_E + a_W^{e,\phi} \Phi_W + a_N^{e,\phi} \Phi_N + a_S^{e,\phi} \Phi_S \quad (30)$$

and

$$\sum a_{\text{NB8}}^{e,\phi} \Phi_{\text{NB8}} = \sum a_{\text{NB4}}^{e,\phi} \Phi_{\text{NB4}} + a_{\text{NE}}^{e,\phi} \Phi_{\text{NE}} + a_{\text{NW}}^{e,\phi} \Phi_{\text{NW}} + a_{\text{SE}}^{e,\phi} \Phi_{\text{SE}} + a_{\text{SW}}^{e,\phi} \Phi_{\text{SW}} \quad (31)$$

Details of the computation of the coefficients in Eqs. (26) to (29) may be found in Section 7.

The nomenclature of the grid generation is given next in Section 3. That nomenclature is needed in the description of geometric interpolations and gradient calculations that follow in Sections 5 and 6.

3 Grid Nomenclature

The typical control volume and its eight neighbours on a structured grid are shown logically in Figure 2. The i and j indices reference each control volume in an organized fashion. The i

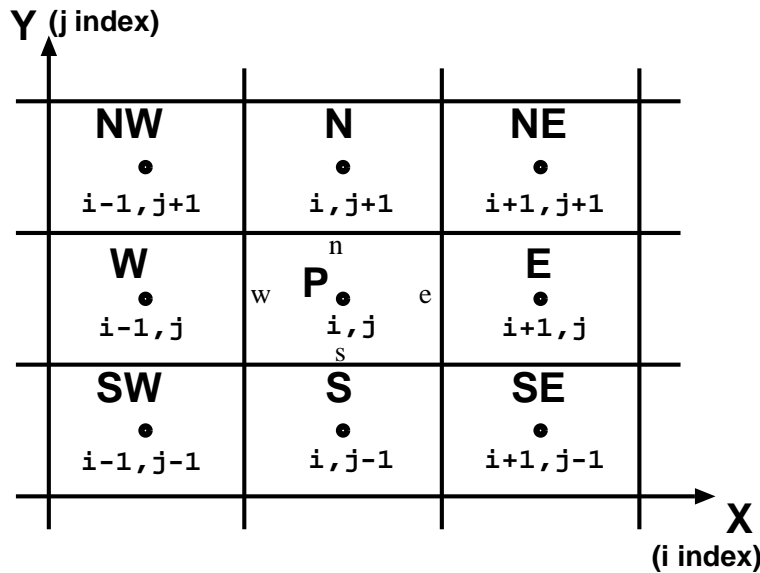


Figure 2: Indexing notation for neighbouring control volumes

index proceeds from IB ($i = 2$) for the first control volume on the west side of the domain to IE ($i = NX + 1$) for the last control volume on the east, where NX is the number of control volumes along the i index. The west to east direction of increasing i index is referred to as the \hat{s} direction. The j index goes from the first control volume on the south, JB ($j = 2$), to the last control volume on the north, JE ($j = NY + 1$), where NY is the number of control volumes along the j index. The south to north direction of increasing j index is referred to as the \hat{t} direction. Each control volume also has a north, south, west and east face as indicated by the lower case letters in the centre control volume labeled “P”. Zero-width control volumes on the boundaries of the domain to implement the boundary conditions. These nodes are referenced by $IB - 1$ on the west, $IE + 1$ on the east, $JB - 1$ on the south, and $JE + 1$ on the north.

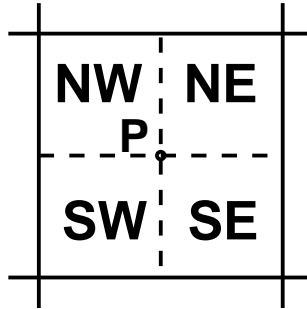


Figure 3: Quadrant notation for a control volume

The quadrant notation used in a each control volume is shown in Figure 3.

The locations of point where x and y coordinate values are stored are labeled in Figure 4. The centre node, “P”, is referenced as “southwest” and the top right corner as “northeast”. The south points are referenced as the north points of the control volume to the south, for example $(XNW_{(i,j-1)}, YNW_{(i,j-1)})$. The west points are referenced as the east points of the control volume to the west. The southwest corner is referenced as $(XNE_{(i-1,j-1)}, YNE_{(i-1,j-1)})$.

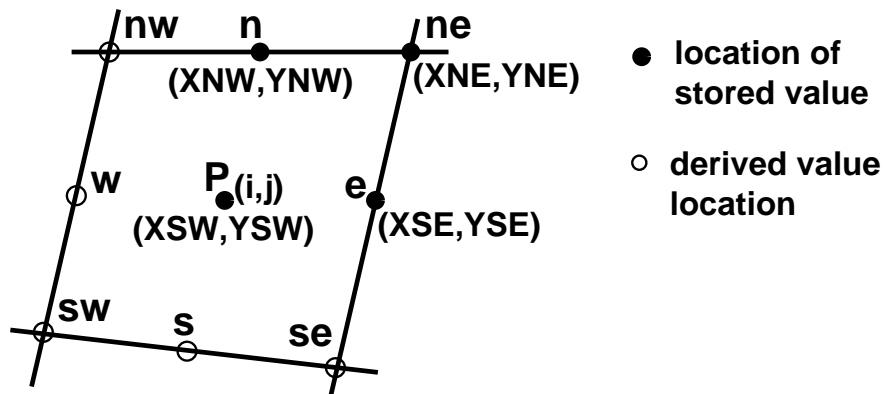


Figure 4: Locations of control volume points

The nomenclature for control volume distances, areas, and volumes is shown in Figure 5. A Cartesian grid is shown for simplicity. The distances are the length between points in the quadrilateral control volume. The quadrants are split into two triangles each. The volume of each triangle is calculated and then the two are added together to get the correct volume for each quadrant. A unit depth is used to compute areas and volumes.

The non-orthogonal grid needs some direction unit vectors and distances defined because the grid will not necessarily be aligned with the Cartesian coordinate directions. As shown in Figure 6, there are separate direction vectors for each face and the central node of the main control volume. The \hat{s} vectors point from west to east and the \hat{t} vectors point from south to north. The vectors on the east face of the present node have subscript “e”, and on the north

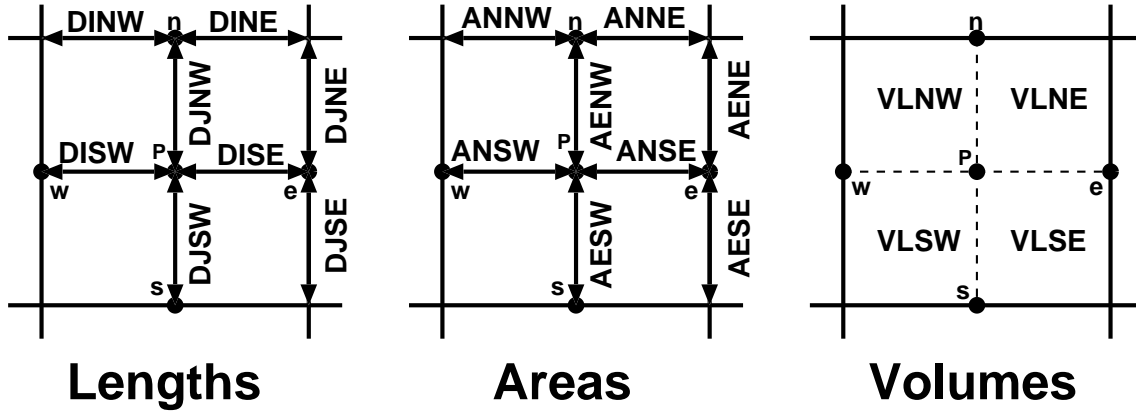


Figure 5: Nomenclature for lengths, areas, and volumes of a control volume

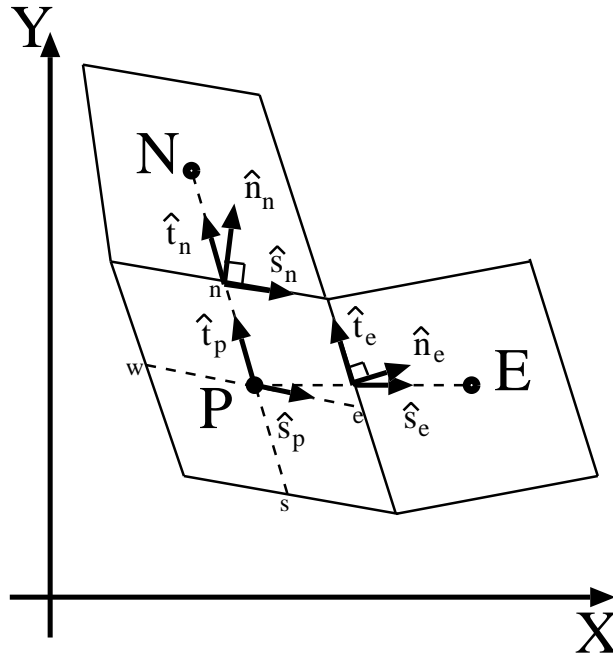


Figure 6: Grid direction vectors

face they have subscript “n”. At an east face, the \hat{t} vector is along the face. Likewise, on a north face, the \hat{s} vector is along the face. The vectors on the west and south of the typical node are referenced by $i - 1$ and $j - 1$ respectively.

Because of the non-orthogonal grid, variables are defined that describe the distance between locations. Figure 7 shows the location of these distance variables for the non-orthogonal grid. The distance between a node and its neighbor to the east, along the \hat{s}_e vector, is defined as:

$$(ds)_{e(i,j)} = \sqrt{(XSW_{(i+1,j)} - XSW_{(i,j)})^2 + (YSW_{(i+1,j)} - YSW_{(i,j)})^2} \quad (32)$$

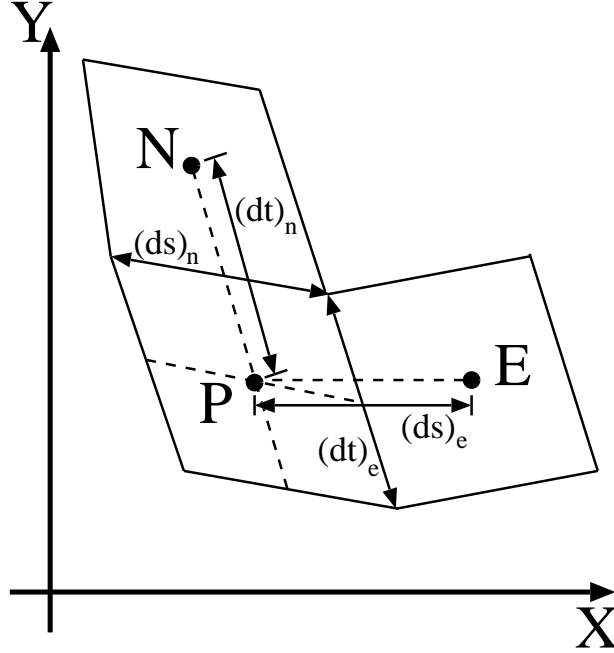


Figure 7: Locations of distance variables

The distance between a node and its neighbor to the north, along the \hat{t}_n vector, is defined as:

$$(dt)_{n(i,j)} = \sqrt{(XSW_{(i,j+1)} - XSW_{(i,j)})^2 + (YSW_{(i,j+1)} - YSW_{(i,j)})^2} \quad (33)$$

The distances $(ds)_n$ and $(dt)_e$ are defined as:

$$(ds)_{n(i,j)} = DINW_{(i,j)} + DINE_{(i,j)} \quad (34)$$

and

$$(dt)_{e(i,j)} = DJSE_{(i,j)} + DJNE_{(i,j)} \quad (35)$$

respectively, and are always equal to the sum of grid quadrant distance variables even if the grid is skewed.

The distances (ds) and (dt) are also evaluated for the nodal location ($(ds)_p$ and $(dt)_p$), the west face ($(dt)_w$), and the south face ($(ds)_s$) analogously to Equations (34) and (35). Likewise, $(ds)_w$ and $(dt)_s$ are defined in a similar fashion to Equations (32) and (33) respectively, although they are not shown in Figure 7.

The north normal unit vector, \hat{n}_n , is defined outward normal to the north face of a control volume as follows:

$$\hat{n}_{n(i,j)} = \frac{-(YNE_{(i,j)} - YNE_{(i-1,j)})}{\sqrt{(XNE_{(i,j)} - XNE_{(i-1,j)})^2 + (YNE_{(i,j)} - YNE_{(i-1,j)})^2}} \hat{i} + \frac{(XNE_{(i,j)} - XNE_{(i-1,j)})}{\sqrt{(XNE_{(i,j)} - XNE_{(i-1,j)})^2 + (YNE_{(i,j)} - YNE_{(i-1,j)})^2}} \hat{j} \quad (36)$$

or in terms of arc lengths

$$\hat{n}_{n(i,j)} = \frac{-(YNE_{(i,j)} - YNE_{(i-1,j)})}{(ds)_n} \hat{i} + \frac{(XNE_{(i,j)} - XNE_{(i-1,j)})}{(ds)_n} \hat{j} \quad (37)$$

where the gradients are defined and evaluated at the north face and converted to normal unit vector notation

$$\hat{n}_{n(i,j)} = \left. \frac{\partial x}{\partial n_n} \right| \hat{i} + \left. \frac{\partial y}{\partial n_n} \right| \hat{j} = n_{xn} \hat{i} + n_{yn} \hat{j} \quad (38)$$

The east normal unit vector, \hat{n}_e , is defined outward normal to the east face of a control volume as follows:

$$\begin{aligned} \hat{n}_{e(i,j)} = & \frac{(YNE_{(i,j)} - YNE_{(i,j-1)})}{\sqrt{(XNE_{(i,j)} - XNE_{(i,j-1)})^2 + (YNE_{(i,j)} - YNE_{(i,j-1)})^2}} \hat{i} \\ & + \frac{-(XNE_{(i,j)} - XNE_{(i,j-1)})}{\sqrt{(XNE_{(i,j)} - XNE_{(i,j-1)})^2 + (YNE_{(i,j)} - YNE_{(i,j-1)})^2}} \hat{j} \end{aligned} \quad (39)$$

or in terms of arc lengths

$$\hat{n}_{e(i,j)} = \frac{(YNE_{(i,j)} - YNE_{(i,j-1)})}{(dt)_e} \hat{i} + \frac{-(XNE_{(i,j)} - XNE_{(i,j-1)})}{(dt)_e} \hat{j} \quad (40)$$

where the gradients are defined and evaluated at the east face and converted to normal unit vector notation

$$\hat{n}_{e(i,j)} = \left. \frac{\partial x}{\partial n_e} \right| \hat{i} + \left. \frac{\partial y}{\partial n_e} \right| \hat{j} = n_{xe} \hat{i} + n_{ye} \hat{j} \quad (41)$$

The west to east geometric grid unit vector for the north face of a control volume, \hat{s}_n , is defined along the line between the northwest and northeast corners of a control volume as follows:

$$\begin{aligned} \hat{s}_{n(i,j)} = & \frac{(XNE_{(i,j)} - XNE_{(i-1,j)})}{\sqrt{(XNE_{(i,j)} - XNE_{(i-1,j)})^2 + (YNE_{(i,j)} - YNE_{(i-1,j)})^2}} \hat{i} \\ & + \frac{(YNE_{(i,j)} - YNE_{(i-1,j)})}{\sqrt{(XNE_{(i,j)} - XNE_{(i-1,j)})^2 + (YNE_{(i,j)} - YNE_{(i-1,j)})^2}} \hat{j} \end{aligned} \quad (42)$$

or in terms of arc lengths

$$\hat{s}_{n(i,j)} = \frac{(XNE_{(i,j)} - XNE_{(i-1,j)})}{(ds)_n} \hat{i} + \frac{(YNE_{(i,j)} - YNE_{(i-1,j)})}{(ds)_n} \hat{j} \quad (43)$$

where the gradients are defined and evaluated at the north face and converted to a west to east geometric grid unit vector notation

$$\hat{s}_{n(i,j)} = \left. \frac{\partial x}{\partial s_n} \right| \hat{i} + \left. \frac{\partial y}{\partial s_n} \right| \hat{j} = s_{xn} \hat{i} + s_{yn} \hat{j} \quad (44)$$

The west to east geometric grid unit vector for the east face of a control volume, \hat{s}_e , is defined along the line between the present node and east node as follows:

$$\hat{s}_{e(i,j)} = \frac{(XSW_{(i+1,j)} - XSW_{(i,j)})}{(ds)_{e(i,j)}} \hat{i} + \frac{(YSW_{(i+1,j)} - YSW_{(i,j)})}{(ds)_{e(i,j)}} \hat{j} \quad (45)$$

where the gradients are defined and evaluated at the east face and converted to a west to east geometric grid unit vector notation

$$\hat{s}_{e(i,j)} = \left. \frac{\partial x}{\partial s} \right|_e \hat{i} + \left. \frac{\partial y}{\partial s} \right|_e \hat{j} = s_{xe} \hat{i} + s_{ye} \hat{j} \quad (46)$$

The west to east geometric grid unit vector for the centre of a control volume, \hat{s}_p , is defined along a line between the centre of the west face and centre of the east face as follows:

$$\begin{aligned} \hat{s}_{p(i,j)} = & \frac{(XSE_{(i,j)} - XSE_{(i-1,j)})}{\sqrt{(XSE_{(i,j)} - XSE_{(i-1,j)})^2 + (YSE_{(i,j)} - YSE_{(i-1,j)})^2}} \hat{i} \\ & + \frac{(YSE_{(i,j)} - YSE_{(i-1,j)})}{\sqrt{(XSE_{(i,j)} - XSE_{(i-1,j)})^2 + (YSE_{(i,j)} - YSE_{(i-1,j)})^2}} \hat{j} \quad (47) \end{aligned}$$

or in terms of arc lengths

$$\hat{s}_{p(i,j)} = \frac{(XSE_{(i,j)} - XSE_{(i-1,j)})}{(ds)_p} \hat{i} + \frac{(YSE_{(i,j)} - YSE_{(i-1,j)})}{(ds)_p} \hat{j} \quad (48)$$

where the gradients are defined and evaluated at the centre of a control volume and converted to a west to east geometric grid unit vector notation

$$\hat{s}_{p(i,j)} = \left. \frac{\partial x}{\partial s} \right|_p \hat{i} + \left. \frac{\partial y}{\partial s} \right|_p \hat{j} = s_{xp} \hat{i} + s_{yp} \hat{j} \quad (49)$$

The south to north geometric grid unit vector for the north face of a control volume, \hat{t}_n , is defined along the line between the present node and north node as follows:

$$\hat{t}_{n(i,j)} = \frac{(XSW_{(i,j+1)} - XSW_{(i,j)})}{(dt)_{n(i,j)}} \hat{i} + \frac{(YSW_{(i,j+1)} - YSW_{(i,j)})}{(dt)_{n(i,j)}} \hat{j} \quad (50)$$

where the gradients are defined and evaluated at the north face and converted to a south to north geometric grid unit vector notation

$$\hat{t}_{n(i,j)} = \left. \frac{\partial x}{\partial t} \right|_n \hat{i} + \left. \frac{\partial y}{\partial t} \right|_n \hat{j} = t_{xn} \hat{i} + t_{yn} \hat{j} \quad (51)$$

The south to north geometric grid unit vector for the east face of a control volume, \hat{t}_e , is defined along the line between the southeast and northeast corners of a control volume as

follows:

$$\hat{t}_{e(i,j)} = \frac{(\text{XNE}_{(i,j)} - \text{XNE}_{(i,j-1)})}{\sqrt{(\text{XNE}_{(i,j)} - \text{XNE}_{(i,j-1)})^2 + (\text{YNE}_{(i,j)} - \text{YNE}_{(i,j-1)})^2}} \hat{i} + \frac{(\text{YNE}_{(i,j)} - \text{YNE}_{(i,j-1)})}{\sqrt{(\text{XNE}_{(i,j)} - \text{XNE}_{(i,j-1)})^2 + (\text{YNE}_{(i,j)} - \text{YNE}_{(i,j-1)})^2}} \hat{j} \quad (52)$$

or in terms of arc lengths

$$\hat{t}_{e(i,j)} = \frac{(\text{XNE}_{(i,j)} - \text{XNE}_{(i,j-1)})}{(dt)_e} \hat{i} + \frac{(\text{YNE}_{(i,j)} - \text{YNE}_{(i,j-1)})}{(dt)_e} \hat{j} \quad (53)$$

where the gradients are defined and evaluated at the east face and converted to a south to north geometric grid unit vector notation

$$\hat{t}_{e(i,j)} = \left. \frac{\partial x}{\partial t} \right|_e \hat{i} + \left. \frac{\partial y}{\partial t} \right|_e \hat{j} = t_{xe} \hat{i} + t_{ye} \hat{j} \quad (54)$$

The south to north geometric grid unit vector for the centre of a control volume, \hat{t}_p , is defined along a line between the centre of the south face and the centre of the north face as follows:

$$\hat{t}_{p(i,j)} = \frac{(\text{XNW}_{(i,j)} - \text{XNW}_{(i,j-1)})}{\sqrt{(\text{XNW}_{(i,j)} - \text{XNW}_{(i,j-1)})^2 + (\text{YNW}_{(i,j)} - \text{YNW}_{(i,j-1)})^2}} \hat{i} + \frac{(\text{YNW}_{(i,j)} - \text{YNW}_{(i,j-1)})}{\sqrt{(\text{XNW}_{(i,j)} - \text{XNW}_{(i,j-1)})^2 + (\text{YNW}_{(i,j)} - \text{YNW}_{(i,j-1)})^2}} \hat{j} \quad (55)$$

or in terms of arc lengths

$$\hat{t}_{p(i,j)} = \frac{(\text{XNW}_{(i,j)} - \text{XNW}_{(i,j-1)})}{(dt)_p} \hat{i} + \frac{(\text{YNW}_{(i,j)} - \text{YNW}_{(i,j-1)})}{(dt)_p} \hat{j} \quad (56)$$

where the gradients are defined and evaluated at the centre of a control volume and converted to a south to north geometric grid unit vector notation

$$\hat{t}_{p(i,j)} = \left. \frac{\partial x}{\partial t} \right|_p \hat{i} + \left. \frac{\partial y}{\partial t} \right|_p \hat{j} = t_{xp} \hat{i} + t_{yp} \hat{j} \quad (57)$$

4 Grid Weights

The grid weights used in Equations (10) to (14) are computed using the grid distances shown in Figure 5. The four face grid weights are computed as follows:

$$\mathcal{W}_{e(i,j)} = \frac{\text{DISW}_{(i+1,j)}}{\text{DISE}_{(i,j)} + \text{DISW}_{(i+1,j)}} \quad (58)$$

$$\mathcal{W}_{n(i,j)} = \frac{\text{DJSW}_{(i+1,j)}}{\text{DJNW}_{(i,j)} + \text{DJSW}_{(i+1,j)}} \quad (59)$$

$$\mathcal{W}_{w(i,j)} = \mathcal{W}_{e(i-1,j)} \quad (60)$$

$$\mathcal{W}_{s(i,j)} = \mathcal{W}_{n(i,j-1)} \quad (61)$$

Note: Are there signs changes on the west and south grid weights?

5 Corner Interpolations

In order to use nine-point solution method, the values at corners are incorporated to estimate derivatives on the faces. The corner vertices are indicated as ne , nw , se , and sw in Figure 1. Geometric interpolations are used to approximate scalar values at corners in a non-uniform grid.

$$\phi_{ne} = C_{ne1}\Phi_P + C_{ne2}\Phi_E + C_{ne3}\Phi_{NE} + C_{ne4}\Phi_N \quad (62)$$

$$\phi_{nw} = C_{nw1}\Phi_P + C_{nw2}\Phi_N + C_{nw3}\Phi_{NW} + C_{nw4}\Phi_W \quad (63)$$

$$\phi_{se} = C_{se1}\Phi_P + C_{se2}\Phi_S + C_{se3}\Phi_{SE} + C_{se4}\Phi_E \quad (64)$$

$$\phi_{sw} = C_{sw1}\Phi_P + C_{sw2}\Phi_W + C_{sw3}\Phi_{SW} + C_{sw4}\Phi_S \quad (65)$$

where the numbering order of C coefficients starts from 1 for node P and goes counter-clockwise around the control volume.

6 Gradient Calculations

On a non-orthogonal grid, the face derivatives in Cartesian x and y directions must be defined in terms of the gradients along the unit vector directions, \hat{s} and \hat{t} as shown in Figure 6. Using the chain rule and Cramer's rule, the derivatives in Cartesian x and y directions on face f are equal to:

$$\left. \frac{\partial \Phi}{\partial x} \right|_f = \mathcal{Y}_{t,f} \left. \frac{\partial \Phi}{\partial s} \right|_f - \mathcal{Y}_{s,f} \left. \frac{\partial \Phi}{\partial t} \right|_f \quad (66)$$

$$\left. \frac{\partial \Phi}{\partial y} \right|_f = \mathcal{X}_{s,f} \left. \frac{\partial \Phi}{\partial t} \right|_f - \mathcal{X}_{t,f} \left. \frac{\partial \Phi}{\partial s} \right|_f \quad (67)$$

where

$$\mathcal{X}_{s,f} = \frac{\left. \frac{\partial x}{\partial s} \right|_f}{\left(\left. \frac{\partial x}{\partial s} \right|_f \left. \frac{\partial y}{\partial t} \right|_f - \left. \frac{\partial x}{\partial t} \right|_f \left. \frac{\partial y}{\partial s} \right|_f \right)} \quad (68)$$

$$\mathcal{X}_{t,f} = \frac{\left. \frac{\partial x}{\partial t} \right|_f}{\left(\left. \frac{\partial x}{\partial s} \right|_f \left. \frac{\partial y}{\partial t} \right|_f - \left. \frac{\partial x}{\partial t} \right|_f \left. \frac{\partial y}{\partial s} \right|_f \right)} \quad (69)$$

$$\mathcal{Y}_{s,f} = \frac{\left. \frac{\partial y}{\partial s} \right|_f}{\left(\left. \frac{\partial x}{\partial s} \right|_f \left. \frac{\partial y}{\partial t} \right|_f - \left. \frac{\partial x}{\partial t} \right|_f \left. \frac{\partial y}{\partial s} \right|_f \right)} \quad (70)$$

$$\mathcal{Y}_{t,f} = \frac{\left. \frac{\partial y}{\partial t} \right|_f}{\left(\left. \frac{\partial x}{\partial s} \right|_f \left. \frac{\partial y}{\partial t} \right|_f - \left. \frac{\partial x}{\partial t} \right|_f \left. \frac{\partial y}{\partial s} \right|_f \right)} \quad (71)$$

and As shown in Figure 6, there are separate direction vectors \hat{s} and \hat{t} for each face (i.e. e , w , n , and s) and central node for the main control volume. Thus, the derivatives in Cartesian directions (Equations (66) and (67)) should be approximated for each face using nodal and corner values.

$$\left. \frac{\partial \Phi}{\partial x} \right|_e = \frac{\mathcal{Y}_{t,e}}{(\delta s)_e} (\Phi_P - \Phi_E) - \frac{\mathcal{Y}_{s,e}}{(\delta t)_e} (\phi_{ne} - \phi_{se}) \quad (72)$$

$$\left. \frac{\partial \Phi}{\partial y} \right|_e = \frac{\mathcal{X}_{t,e}}{(\delta s)_e} (\Phi_E - \Phi_P) + \frac{\mathcal{X}_{s,e}}{(\delta t)_e} (\phi_{ne} - \phi_{se}) \quad (73)$$

$$\left. \frac{\partial \Phi}{\partial x} \right|_w = \frac{\mathcal{Y}_{t,w}}{(\delta s)_w} (\Phi_W - \Phi_P) - \frac{\mathcal{Y}_{s,w}}{(\delta t)_w} (\phi_{nw} - \phi_{sw}) \quad (74)$$

$$\left. \frac{\partial \Phi}{\partial y} \right|_w = \frac{\mathcal{X}_{t,w}}{(\delta t)_w} (\Phi_P - \Phi_W) + \frac{\mathcal{X}_{s,w}}{(\delta s)_w} (\phi_{nw} - \phi_{sw}) \quad (75)$$

$$\left. \frac{\partial \Phi}{\partial x} \right|_n = \frac{\mathcal{Y}_{s,n}}{(\delta s)_n} (\Phi_N - \Phi_P) + \frac{\mathcal{Y}_{t,n}}{(\delta t)_n} (\phi_{ne} - \phi_{nw}) \quad (76)$$

$$\left. \frac{\partial \Phi}{\partial y} \right|_n = \frac{\mathcal{X}_{s,n}}{(\delta t)_n} (\Phi_P - \Phi_N) - \frac{\mathcal{X}_{t,n}}{(\delta s)_n} (\phi_{ne} - \phi_{nw}) \quad (77)$$

$$\left. \frac{\partial \Phi}{\partial x} \right|_s = \frac{\mathcal{Y}_{s,s}}{(\delta s)_s} (\Phi_P - \Phi_S) + \frac{\mathcal{Y}_{t,s}}{(\delta t)_s} (\phi_{se} - \phi_{sw}) \quad (78)$$

$$\left. \frac{\partial \Phi}{\partial y} \right|_s = \frac{\mathcal{X}_{s,s}}{(\delta t)_s} (\Phi_S - \Phi_P) - \frac{\mathcal{X}_{t,s}}{(\delta s)_s} (\phi_{se} - \phi_{sw}) \quad (79)$$

Note: Need to add equations for normal-direction derivatives.

7 Coefficients of the Coupled Algebraic Equations

7.1 Continuity

Substituting Equations (62) to (65) into Equations (72) to (79) for the pressure variable ($\Phi = P$), the pressure gradients on the faces in Equations (10) and (11) are approximated in terms of nodal values. Now, the coefficients of continuity equation (Equation (28)) are:

$$a_P^{c,u} = a_P^{c,v} = \sum (\rho A_f \mathcal{W}_f) = \rho A_e \mathcal{W}_e + \rho A_w \mathcal{W}_w + \rho A_n \mathcal{W}_n + \rho A_s \mathcal{W}_s \quad (80)$$

$$a_F^{c,u} = a_F^{c,v} = \rho A_f (1 - \mathcal{W}_f) \quad (81)$$

$$\begin{aligned} a_P^{c,p} = & -\rho A_e \hat{d}_e^u \left[\frac{\mathcal{Y}_{t,e}}{(\delta s)_e} - \frac{\mathcal{Y}_{s,e}}{(\delta t)_e} (C_{ne1} - C_{se1}) \right] + \rho A_w \hat{d}_w^u \left[\frac{\mathcal{Y}_{t,w}}{(\delta s)_w} + \frac{\mathcal{Y}_{s,w}}{(\delta t)_w} (C_{nw1} - C_{sw1}) \right] \\ & + \rho A_n \hat{d}_n^u \left[\frac{\mathcal{Y}_{s,n}}{(\delta t)_n} - \frac{\mathcal{Y}_{t,n}}{(\delta s)_n} (C_{ne1} - C_{nw1}) \right] - \rho A_s \hat{d}_s^u \left[\frac{\mathcal{Y}_{s,s}}{(\delta t)_s} + \frac{\mathcal{Y}_{t,s}}{(\delta s)_s} (C_{se1} - C_{sw1}) \right] \\ & + \rho A_e \hat{d}_e^v \left[\frac{\mathcal{X}_{t,e}}{(\delta s)_e} - \frac{\mathcal{X}_{s,e}}{(\delta t)_e} (C_{ne1} - C_{se1}) \right] - \rho A_w \hat{d}_w^v \left[\frac{\mathcal{X}_{t,w}}{(\delta s)_w} + \frac{\mathcal{X}_{s,w}}{(\delta t)_w} (C_{nw1} - C_{sw1}) \right] \\ & - \rho A_n \hat{d}_n^v \left[\frac{\mathcal{X}_{s,n}}{(\delta t)_n} - \frac{\mathcal{X}_{t,n}}{(\delta s)_n} (C_{ne1} - C_{nw1}) \right] + \rho A_s \hat{d}_s^v \left[\frac{\mathcal{X}_{s,s}}{(\delta t)_s} + \frac{\mathcal{X}_{t,s}}{(\delta s)_s} (C_{se1} - C_{sw1}) \right] \end{aligned} \quad (82)$$

$$\begin{aligned} a_E^{c,p} = & \rho A_e \left(\hat{d}_e^u \frac{\mathcal{Y}_{t,e}}{(\delta s)_e} - \hat{d}_e^v \frac{\mathcal{X}_{t,e}}{(\delta s)_e} \right) - \rho A_n \left(\hat{d}_n^u \frac{\mathcal{Y}_{t,n}}{(\delta s)_n} - \hat{d}_n^v \frac{\mathcal{X}_{t,n}}{(\delta s)_n} \right) C_{ne2} \\ & - \rho A_s \left(\hat{d}_s^u \frac{\mathcal{Y}_{t,s}}{(\delta s)_s} + \hat{d}_s^v \frac{\mathcal{X}_{t,s}}{(\delta s)_s} \right) C_{se4} - \rho A_e \left(\hat{d}_e^u \frac{\mathcal{Y}_{s,e}}{(\delta t)_e} + \hat{d}_e^v \frac{\mathcal{X}_{s,e}}{(\delta t)_e} \right) (C_{ne2} - C_{se4}) \end{aligned} \quad (83)$$

$$\begin{aligned} a_W^{c,p} = & -\rho A_w \left(\hat{d}_w^u \frac{\mathcal{Y}_{t,w}}{(\delta s)_w} + \hat{d}_w^v \frac{\mathcal{X}_{t,w}}{(\delta s)_w} \right) + \rho A_n \left(\hat{d}_n^u \frac{\mathcal{Y}_{t,n}}{(\delta s)_n} - \hat{d}_n^v \frac{\mathcal{X}_{t,n}}{(\delta s)_n} \right) C_{nw4} \\ & + \rho A_s \left(\hat{d}_s^u \frac{\mathcal{Y}_{t,s}}{(\delta s)_s} - \hat{d}_s^v \frac{\mathcal{X}_{t,s}}{(\delta s)_s} \right) C_{sw2} + \rho A_w \left(\hat{d}_w^u \frac{\mathcal{Y}_{s,w}}{(\delta t)_w} - \hat{d}_w^v \frac{\mathcal{X}_{s,w}}{(\delta t)_w} \right) (C_{nw4} - C_{sw2}) \end{aligned} \quad (84)$$

$$\begin{aligned} a_N^{c,p} = & -\rho A_n \left(\hat{d}_n^u \frac{\mathcal{Y}_{s,n}}{(\delta t)_n} + \hat{d}_n^v \frac{\mathcal{X}_{s,n}}{(\delta t)_n} \right) + \rho A_e \left(\hat{d}_e^u \frac{\mathcal{Y}_{s,e}}{(\delta t)_e} - \hat{d}_e^v \frac{\mathcal{X}_{s,e}}{(\delta t)_e} \right) C_{ne4} \\ & + \rho A_w \left(\hat{d}_w^u \frac{\mathcal{Y}_{s,w}}{(\delta t)_w} - \hat{d}_w^v \frac{\mathcal{X}_{s,w}}{(\delta t)_w} \right) C_{nw2} - \rho A_n \left(\hat{d}_n^u \frac{\mathcal{Y}_{t,n}}{(\delta s)_e} - \hat{d}_n^v \frac{\mathcal{X}_{t,n}}{(\delta s)_e} \right) (C_{ne4} - C_{nw2}) \end{aligned} \quad (85)$$

$$\begin{aligned} a_S^{c,p} = & \rho A_s \left(\hat{d}_s^u \frac{\mathcal{Y}_{s,s}}{(\delta t)_s} - \hat{d}_s^v \frac{\mathcal{X}_{s,s}}{(\delta t)_s} \right) - \rho A_e \left(\hat{d}_e^u \frac{\mathcal{Y}_{s,e}}{(\delta t)_e} - \hat{d}_e^v \frac{\mathcal{X}_{s,e}}{(\delta t)_e} \right) C_{se2} \\ & - \rho A_w \left(\hat{d}_w^u \frac{\mathcal{Y}_{s,w}}{(\delta t)_w} - \hat{d}_w^v \frac{\mathcal{X}_{s,w}}{(\delta t)_w} \right) C_{sw4} - \rho A_s \left(\hat{d}_s^u \frac{\mathcal{Y}_{t,s}}{(\delta s)_s} - \hat{d}_s^v \frac{\mathcal{X}_{t,s}}{(\delta s)_s} \right) (C_{se2} - C_{sw4}) \end{aligned} \quad (86)$$

$$a_{NE}^{c,p} = \left(\rho A_e \hat{d}_e^u \frac{\mathcal{Y}_{s,e}}{(\delta t)_e} - \rho A_e \hat{d}_e^v \frac{\mathcal{X}_{s,e}}{(\delta t)_e} - \rho A_n \hat{d}_n^u \frac{\mathcal{Y}_{t,n}}{(\delta s)_n} + \rho A_n \hat{d}_n^v \frac{\mathcal{X}_{t,n}}{(\delta s)_n} \right) C_{ne3} \quad (87)$$

$$a_{NW}^{c,p} = \left(\rho A_w \hat{d}_w^u \frac{\mathcal{Y}_{s,w}}{(\delta t)_w} - \rho A_w \hat{d}_w^v \frac{\mathcal{X}_{s,w}}{(\delta t)_w} + \rho A_n \hat{d}_n^u \frac{\mathcal{Y}_{t,n}}{(\delta s)_n} - \rho A_n \hat{d}_n^v \frac{\mathcal{X}_{t,n}}{(\delta s)_n} \right) C_{nw3} \quad (88)$$

$$a_{SE}^{c,p} = - \left(\rho A_e \hat{d}_e^u \frac{\mathcal{Y}_{s,e}}{(\delta t)_e} - \rho A_e \hat{d}_e^v \frac{\mathcal{X}_{s,e}}{(\delta t)_e} + \rho A_s \hat{d}_s^u \frac{\mathcal{Y}_{t,s}}{(\delta s)_s} - \rho A_s \hat{d}_s^v \frac{\mathcal{X}_{t,s}}{(\delta s)_s} \right) C_{se3} \quad (89)$$

$$a_{SW}^{c,p} = - \left(\rho A_w \hat{d}_w^u \frac{\mathcal{Y}_{s,w}}{(\delta t)_w} - \rho A_w \hat{d}_w^v \frac{\mathcal{X}_{s,w}}{(\delta t)_w} - \rho A_s \hat{d}_s^u \frac{\mathcal{Y}_{t,s}}{(\delta s)_s} + \rho A_s \hat{d}_s^v \frac{\mathcal{X}_{t,s}}{(\delta s)_s} \right) C_{sw3} \quad (90)$$

$$b_P^c = \sum \rho A_f (\tilde{b}_f^u + \tilde{b}_f^v) \quad (91)$$

7.2 X-Momentum

Using geometric directions for each face of the typical control volume, the diffusion terms in X-momentum equation are approximated in terms of nodal values. In Equation (26), the U velocity coefficients of main node ($a_P^{u,u}$) and its eight neighbour nodes ($a_{NB8}^{u,u}$) are as follows:

$$\begin{aligned} a_P^{u,u} = & \left(\frac{\rho V_P}{\Delta t} \right) - (0.5 - \alpha_e) \dot{m}_e + (0.5 + \alpha_w) \dot{m}_w - (0.5 - \alpha_n) \dot{m}_n + (0.5 + \alpha_s) \dot{m}_s \\ & + \frac{D_e^u \beta_e}{\hat{n}_e \cdot \hat{s}_e} + \frac{D_w^u \beta_w}{\hat{n}_w \cdot \hat{s}_w} + \frac{D_n^u \beta_n}{\hat{n}_n \cdot \hat{s}_n} + \frac{D_s^u \beta_s}{\hat{n}_s \cdot \hat{s}_s} + D_e^u \beta_e \gamma_{x,e} (C_{ne1} - C_{se1}) \\ & - D_w^u \beta_w \gamma_{x,w} (C_{nw1} - C_{sw1}) + D_n^u \beta_n \gamma_{y,n} (C_{ne1} - C_{nw1}) - D_s^u \beta_s \gamma_{y,s} (C_{se1} - C_{sw1}) \end{aligned} \quad (92)$$

$$\begin{aligned} a_E^{u,u} = & (0.5 - \alpha_e) \dot{m}_e - \frac{D_e^u \beta_e}{\hat{n}_e \cdot \hat{s}_e} + D_n^u \beta_n \gamma_{y,n} C_{ne2} - D_s^u \beta_s \gamma_{y,s} C_{se4} \\ & + D_e^u \beta_e \gamma_{x,e} (C_{ne2} - C_{se4}) \end{aligned} \quad (93)$$

$$\begin{aligned} a_W^{u,u} = & - (0.5 + \alpha_w) \dot{m}_w - \frac{D_w^u \beta_w}{\hat{n}_w \cdot \hat{s}_w} - D_n^u \beta_n \gamma_{y,n} C_{nw4} + D_s^u \beta_s \gamma_{y,s} C_{sw2} \\ & - D_w^u \beta_w \gamma_{x,w} (C_{nw4} - C_{sw2}) \end{aligned} \quad (94)$$

$$\begin{aligned} a_N^{u,u} = & (0.5 - \alpha_n) \dot{m}_n - \frac{D_n^u \beta_n}{\hat{n}_n \cdot \hat{s}_n} + D_e^u \beta_e \gamma_{x,e} C_{ne4} - D_w^u \beta_w \gamma_{x,w} C_{nw2} \\ & + D_n^u \beta_n \gamma_{y,n} (C_{ne4} - C_{nw2}) \end{aligned} \quad (95)$$

$$\begin{aligned} a_S^{u,u} = & - (0.5 + \alpha_s) \dot{m}_s - \frac{D_s^u \beta_s}{\hat{n}_s \cdot \hat{s}_s} - D_e^u \beta_e \gamma_{x,e} C_{se2} + D_w^u \beta_w \gamma_{x,w} C_{sw4} \\ & - D_s^u \beta_s \gamma_{y,s} (C_{se2} - C_{sw4}) \end{aligned} \quad (96)$$

$$a_{NE}^{u,u} = (D_e^u \beta_e \gamma_{x,e} + D_w^u \beta_w \gamma_{y,n}) C_{ne3} \quad (97)$$

$$a_{NW}^{u,u} = - (D_w^u \beta_w \gamma_{x,w} + D_n^u \beta_n \gamma_{y,n}) C_{nw3} \quad (98)$$

$$a_{SE}^{u,u} = - (D_e^u \beta_e \gamma_{x,e} + D_n^u \beta_n \gamma_{y,s}) C_{se3} \quad (99)$$

$$a_{SW}^{u,u} = (D_w^u \beta_w \gamma_{x,w} + D_s^u \beta_s \gamma_{y,s}) C_{sw3} \quad (100)$$

where

$$D_e^u = \frac{\mu A_e}{(\delta s)_e} \quad D_w^u = \frac{\mu A_w}{(\delta s)_w} \quad D_n^u = \frac{\mu A_n}{(\delta s)_n} \quad D_s^u = \frac{\mu A_s}{(\delta s)_s} \quad (101)$$

$$\gamma_{x,f} = \frac{(\delta s)_f \hat{t}_f \cdot \hat{s}_f}{(\delta t)_f \hat{n}_f \cdot \hat{s}_f} \quad \gamma_{y,f} = \frac{(\delta t)_f \hat{t}_f \cdot \hat{s}_f}{(\delta s)_f \hat{n}_f \cdot \hat{t}_f} \quad (102)$$

The pressure terms in the momentum equations are implicitly discretised and simultaneously solved in a fully coupled manner. For this reason, the approximations of Cartesian derivatives on main control volume faces (*i.e.* Equations (66) and (67)), are written for the centre node P . Using geometric interpolation for the face pressures, the pressure coefficients of main node ($a_P^{u,p}$) and its four neighbours ($a_{\text{NB}4}^{u,p}$) in Equation (26) are derived as follows:

$$a_P^{u,p} = \mathbb{V}_P \frac{\mathcal{Y}_{t,P}}{(\delta s)_p} (\mathcal{W}_e - \mathcal{W}_w) - \mathbb{V}_P \frac{\mathcal{Y}_{s,P}}{(\delta t)_p} (\mathcal{W}_n - \mathcal{W}_s) \quad (103)$$

$$a_E^{u,p} = \mathbb{V}_P \frac{\mathcal{Y}_{t,P}}{(\delta s)_p} (1 - \mathcal{W}_e) \quad (104)$$

$$a_W^{u,p} = -\mathbb{V}_P \frac{\mathcal{Y}_{t,P}}{(\delta s)_p} (1 - \mathcal{W}_w) \quad (105)$$

$$a_N^{u,p} = -\mathbb{V}_P \frac{\mathcal{Y}_{s,P}}{(\delta t)_p} (1 - \mathcal{W}_n) \quad (106)$$

$$a_S^{u,p} = \mathbb{V}_P \frac{\mathcal{Y}_{s,P}}{(\delta t)_p} (1 - \mathcal{W}_s) \quad (107)$$

If the buoyancy term is implicitly discretised, the temperature coefficient in Equation (26) is:

$$a_P^{u,t} = -\mathbb{V}_P g_x \beta \rho \quad (108)$$

It is obvious that $a_P^{u,t} = 0$, if no buoyancy forces are considered in the flow or they are treated explicitly.

Considering an implicit role for the buoyancy term, the right hand side of Equation (26) is:

$$b_P^u = \left(\frac{\rho \mathbb{V}_P}{\Delta t} \right) U_P^o - \mathbb{V}_P g_x \beta \rho T_{\text{ref}} \quad (109)$$

7.3 Y-Momentum

Each term in the y -momentum equation is derived in the same manner as was used for the x -momentum equation. The corresponding coefficients for Equation (27) are expressed as:

$$a_P^{v,v} = a_P^{u,u} \quad a_{nb}^{v,v} = a_{nb}^{u,u} \quad (110)$$

The diffusion coefficient for v as the same as those for u :

$$D_e^v = \frac{\mu A_e}{(\delta s)_e} \quad D_w^v = \frac{\mu A_w}{(\delta s)_w} \quad D_n^v = \frac{\mu A_n}{(\delta s)_n} \quad D_s^v = \frac{\mu A_s}{(\delta s)_s} \quad (111)$$

$$a_P^{v,p} = \mathbb{V}_P \frac{\mathcal{X}_{s,P}}{(\delta t)_p} (\mathcal{W}_n - \mathcal{W}_s) - \mathbb{V}_P \frac{\mathcal{X}_{t,P}}{(\delta s)_p} (\mathcal{W}_e - \mathcal{W}_w) \quad (112)$$

$$a_E^{v,p} = -V_P \frac{\mathcal{X}_{t,P}}{(\delta s)_p} (1 - \mathcal{W}_e) \quad (113)$$

$$a_W^{v,p} = V_P \frac{\mathcal{X}_{t,P}}{(\delta s)_p} (1 - \mathcal{W}_w) \quad (114)$$

$$a_N^{v,p} = V_P \frac{\mathcal{X}_{s,P}}{(\delta t)_p} (1 - \mathcal{W}_n) \quad (115)$$

$$a_S^{v,p} = -V_P \frac{\mathcal{X}_{s,P}}{(\delta t)_p} (1 - \mathcal{W}_s) \quad (116)$$

$$a_P^{v,t} = -V_P g_y \beta \rho \quad (117)$$

$$b_P^v = \left(\frac{\rho V_P}{\Delta t} \right) V_P^o - V_P g_y \beta \rho T_{\text{ref}} \quad (118)$$

7.4 Energy

The derivation of $a_P^{t,t}$ and $a_{nb}^{t,t}$ is analogous to that for the U velocity coefficient in X-momentum equation using $\frac{k}{C_p}$ instead of μ in D_f coefficients.

The Newton-Raphson linearisation of the advection terms couples the energy equation with the velocity and pressure fields. The derivation of velocity and pressure terms in the energy equation is similar to the derivation of continuity equation coefficients.

$$a_P^{t,u} = a_P^{t,v} = \sum (\rho A_f \mathcal{W}_f T_f^o) = \rho A_e \mathcal{W}_e T_e^o + \rho A_w \mathcal{W}_w T_w^o + \rho A_n \mathcal{W}_n T_n^o + \rho A_s \mathcal{W}_s T_s^o \quad (119)$$

$$a_F^{t,u} = a_F^{t,v} = \rho A_f (1 - \mathcal{W}_f T_f^o) \quad (120)$$

$$\begin{aligned} a_P^{t,p} = & \rho A_e \left\{ -\hat{d}_e^u \left[\frac{\mathcal{Y}_{t,e}}{(\delta s)_e} - \frac{\mathcal{Y}_{s,e}}{(\delta t)_e} (C_{ne1} - C_{se1}) \right] + \hat{d}_e^v \left[\frac{\mathcal{X}_{t,e}}{(\delta s)_e} - \frac{\mathcal{X}_{s,e}}{(\delta t)_e} (C_{ne1} - C_{se1}) \right] \right\} T_e^o \\ & + \rho A_w \left\{ \hat{d}_w^u \left[\frac{\mathcal{Y}_{t,w}}{(\delta s)_w} + \frac{\mathcal{Y}_{s,w}}{(\delta t)_w} (C_{nw1} - C_{sw1}) \right] - \hat{d}_w^v \left[\frac{\mathcal{X}_{t,w}}{(\delta s)_w} + \frac{\mathcal{X}_{s,w}}{(\delta t)_w} (C_{nw1} - C_{sw1}) \right] \right\} T_w^o \\ & + \rho A_n \left\{ \hat{d}_n^u \left[\frac{\mathcal{Y}_{t,n}}{(\delta t)_n} - \frac{\mathcal{Y}_{s,n}}{(\delta s)_n} (C_{ne1} - C_{nw1}) \right] - \hat{d}_n^v \left[\frac{\mathcal{X}_{t,n}}{(\delta t)_n} - \frac{\mathcal{X}_{s,n}}{(\delta s)_n} (C_{ne1} - C_{nw1}) \right] \right\} T_n^o \\ & + \rho A_s \left\{ -\hat{d}_s^u \left[\frac{\mathcal{Y}_{s,s}}{(\delta t)_s} + \frac{\mathcal{Y}_{t,s}}{(\delta s)_s} (C_{se1} - C_{sw1}) \right] + \hat{d}_s^v \left[\frac{\mathcal{X}_{s,s}}{(\delta t)_s} + \frac{\mathcal{X}_{t,s}}{(\delta s)_s} (C_{se1} - C_{sw1}) \right] \right\} T_s^o \quad (121) \end{aligned}$$

$$\begin{aligned} a_E^{t,p} = & \rho A_e \left(\hat{d}_e^u \frac{\mathcal{Y}_{t,e}}{(\delta s)_e} - \hat{d}_e^v \frac{\mathcal{X}_{t,e}}{(\delta s)_e} \right) T_e^o - \rho A_n \left(\hat{d}_n^u \frac{\mathcal{Y}_{t,n}}{(\delta s)_n} - \hat{d}_n^v \frac{\mathcal{X}_{t,n}}{(\delta s)_n} \right) C_{ne2} T_n^o \\ & - \rho A_s \left(\hat{d}_s^u \frac{\mathcal{Y}_{t,s}}{(\delta s)_s} + \hat{d}_s^v \frac{\mathcal{X}_{t,s}}{(\delta s)_s} \right) C_{se4} T_s^o - \rho A_e \left(\hat{d}_e^u \frac{\mathcal{Y}_{s,e}}{(\delta t)_e} + \hat{d}_e^v \frac{\mathcal{X}_{s,e}}{(\delta t)_e} \right) (C_{ne2} - C_{se4}) T_e^o \quad (122) \end{aligned}$$

$$\begin{aligned} a_W^{t,p} = & \rho A_w \left(-\hat{d}_w^u \frac{\mathcal{Y}_{t,w}}{(\delta s)_w} + \hat{d}_w^v \frac{\mathcal{X}_{t,w}}{(\delta s)_w} \right) T_w^o + \rho A_n \left(\hat{d}_n^u \frac{\mathcal{Y}_{t,n}}{(\delta s)_n} - \hat{d}_n^v \frac{\mathcal{X}_{t,n}}{(\delta s)_n} \right) C_{nw4} T_n^o \\ & + \rho A_s \left(\hat{d}_s^u \frac{\mathcal{Y}_{t,s}}{(\delta s)_s} - \hat{d}_s^v \frac{\mathcal{X}_{t,s}}{(\delta s)_s} \right) C_{sw2} T_s^o + \rho A_w \left(\hat{d}_w^u \frac{\mathcal{Y}_{s,w}}{(\delta t)_w} - \hat{d}_w^v \frac{\mathcal{X}_{s,w}}{(\delta t)_w} \right) (C_{nw4} - C_{sw2}) T_w^o \quad (123) \end{aligned}$$

$$\begin{aligned}
 a_N^{t,p} = & \rho A_n \left(-\hat{d}_n^u \frac{\mathcal{Y}_{s,n}}{(\delta t)_n} + \hat{d}_n^v \frac{\mathcal{X}_{s,n}}{(\delta t)_n} \right) T_n^o + \rho A_e \left(\hat{d}_e^u \frac{\mathcal{Y}_{s,e}}{(\delta t)_e} - \hat{d}_e^v \frac{\mathcal{X}_{s,e}}{(\delta t)_e} \right) C_{ne4} T_e^o \\
 & + \rho A_w \left(\hat{d}_w^u \frac{\mathcal{Y}_{s,w}}{(\delta t)_w} - \hat{d}_w^v \frac{\mathcal{X}_{s,w}}{(\delta t)_w} \right) C_{nw2} T_w^o - \rho A_n \left(\hat{d}_n^u \frac{\mathcal{Y}_{t,n}}{(\delta s)_e} - \hat{d}_n^v \frac{\mathcal{X}_{t,n}}{(\delta s)_e} \right) (C_{ne4} - C_{nw2}) T_n^o
 \end{aligned} \tag{124}$$

$$\begin{aligned}
 a_S^{t,p} = & \rho A_s \left(\hat{d}_s^u \frac{\mathcal{Y}_{s,s}}{(\delta t)_s} - \hat{d}_s^v \frac{\mathcal{X}_{s,s}}{(\delta t)_s} \right) T_s^o - \rho A_e \left(\hat{d}_e^u \frac{\mathcal{Y}_{s,e}}{(\delta t)_e} - \hat{d}_e^v \frac{\mathcal{X}_{s,e}}{(\delta t)_e} \right) C_{se2} T_e^o \\
 & - \rho A_w \left(\hat{d}_w^u \frac{\mathcal{Y}_{s,w}}{(\delta t)_w} - \hat{d}_w^v \frac{\mathcal{X}_{s,w}}{(\delta t)_w} \right) C_{sw4} T_w^o - \rho A_s \left(\hat{d}_s^u \frac{\mathcal{Y}_{t,s}}{(\delta s)_s} - \hat{d}_s^v \frac{\mathcal{X}_{t,s}}{(\delta s)_s} \right) (C_{se2} - C_{sw4}) T_s^o
 \end{aligned} \tag{125}$$

$$a_{NE}^{t,p} = \left[\rho A_e \left(\hat{d}_e^u \frac{\mathcal{Y}_{s,e}}{(\delta t)_e} - \hat{d}_e^v \frac{\mathcal{X}_{s,e}}{(\delta t)_e} \right) T_e^o - \rho A_n \left(\hat{d}_n^u \frac{\mathcal{Y}_{t,n}}{(\delta s)_n} + \hat{d}_n^v \frac{\mathcal{X}_{t,n}}{(\delta s)_n} \right) T_n^o \right] C_{ne3} \tag{126}$$

$$a_{NW}^{t,p} = \left[\rho A_w \left(\hat{d}_w^u \frac{\mathcal{Y}_{s,w}}{(\delta t)_w} - \hat{d}_w^v \frac{\mathcal{X}_{s,w}}{(\delta t)_w} \right) T_w^o + \rho A_n \left(\hat{d}_n^u \frac{\mathcal{Y}_{t,n}}{(\delta s)_n} - \hat{d}_n^v \frac{\mathcal{X}_{t,n}}{(\delta s)_n} \right) T_n^o \right] C_{nw3} \tag{127}$$

$$a_{SE}^{t,p} = - \left[\rho A_e \left(\hat{d}_e^u \frac{\mathcal{Y}_{s,e}}{(\delta t)_e} - \hat{d}_e^v \frac{\mathcal{X}_{s,e}}{(\delta t)_e} \right) T_e^o + \rho A_s \left(\hat{d}_s^u \frac{\mathcal{Y}_{t,s}}{(\delta s)_s} - \hat{d}_s^v \frac{\mathcal{X}_{t,s}}{(\delta s)_s} \right) T_s^o \right] C_{se3} \tag{128}$$

$$a_{SW}^{t,p} = - \left[\rho A_w \left(\hat{d}_w^u \frac{\mathcal{Y}_{s,w}}{(\delta t)_w} - \hat{d}_w^v \frac{\mathcal{X}_{s,w}}{(\delta t)_w} \right) T_w^o - \rho A_s \left(\hat{d}_s^u \frac{\mathcal{Y}_{t,s}}{(\delta s)_s} + \hat{d}_s^v \frac{\mathcal{X}_{t,s}}{(\delta s)_s} \right) T_s^o \right] C_{sw3} \tag{129}$$

$$b_P^t = \left(\frac{\rho V_P}{\Delta t} \right) T_P^o + \sum \rho A_f \left(\tilde{b}_f^u + \tilde{b}_f^v + \dot{m}_f^o \right) T_f^o \tag{130}$$

8 References

- [1] S. V. Patankar, *Numerical Heat Transfer and Fluid Flow*, Hemisphere, Washington, 1980.
- [2] C. M. Rhie and W. L. Chow, Numerical Study of the Turbulent Flow Past an Airfoil with Trailing Edge Separation, *AIAA Journal*, vol. 21, pp. 1525–1532, 1983.
- [3] B. Yu, Y. Kawaguchi, W. Tao, and H. Ozoe, Checkerboard pressure predictions due to the underrelaxation factor and time step size for a nonstaggered grid with momentum interpolation method, *Numerical Heat Transfer, Part B (Fundamentals)*, vol. 41, pp. 85–94, 2002.
- [4] P. F. Galpin and G. D. Raithby, Numerical Solution of Problems in Incompressible Fluid Flow: Treatment of the Temperature-Velocity Coupling, *Numerical Heat Transfer*, vol. 10, pp. 105–129, 1986.
- [5] G. D. Raithby and G. E. Schneider, Elliptic Systems: Finite-Difference Method II, in W. J. Minkowycz, E. M. Sparrow, G. E. Schneider, and R. H. Pletcher (eds.), *Handbook of Numerical Heat Transfer*, John Wiley & Sons, 1988.